Realization of quantum-mechanical weak values of observables using entangled photons

G. S. Agarwal and P. K. Pathak
Department of Physics, Oklahoma State University, Stillwater, Oklahoma 74078, USA
(Received 11 December 2006; published 12 March 2007)

We present a scheme for realization of quantum-mechanical weak values of observables using entangled photons produced in parametric down-conversion. We consider the case when the signal and idler modes are respectively in a coherent state and vacuum. We use a low-efficiency detector to detect the photons in the idler mode. This weak detection leads to a large displacement and fluctuations in the signal field's quantum state which can be studied by monitoring the photon number and quadrature distributions. This also demonstrates the effect of weak measurement of one partner on its twin.

DOI: 10.1103/PhysRevA.75.032108 PACS number(s): 03.65.Ta, 03.67.−a, 42.50.Xa

I. INTRODUCTION

In a remarkable paper Aharonov, Albert, and Vaidman [1] discovered that under conditions of very weak coupling between the system and the measuring device the uncertainty in a single measurement could be very large compared with the separation between the eigenvalues of the observable. This is quite a departure from the usual idea of projective measurements where the measurement projects on to one of the eigenvalues [2]. Aharonov *et al.*'s proposal was further clarified by several authors [3–6]. In particular, Duck *et al.* [3] also suggested an optical experiment to verify the idea. Such an optical experiment was performed by Ritchie *et al.* [7]. This experiment uses the classical light source like a laser beam; a birefringent medium and the pre and post selection of the polarization of the transmitted beam. The experiment is well explained using classical physics as discussed in the paper by Ritchie *et al.* [7]. It would therefore be interesting to find situations that are strictly quantum in nature even though the experiment of Ritchie *et al.* was repeated at the single-photon level and in particular weak values of the photon arrival times were measured [8]. Further weak values of the polarization of a single photon were reported [9]. In this paper we show how the idea of Aharonov *et al.* could be realized using entangled photons produced in the process of parametric down-conversion, thus making their proposal within the reach of current experiments. We specifically discuss the weak values associated with the measurement of the photon number and the quadrature of the signal field. We also discuss how the weak values are reflected in the fluctuations of the state of the signal field. Our explicit result for the state of the signal field shows the role of quantum interferences in the weak values of the observables. We require two ingredients for the observation—high value of the squeezing parameter and a well-controlled detector. Both of these are feasible. We note that Zambra *et al.* [10] have very successfully demonstrated the application of avalanche detectors for the reconstruction of photon statistics. Further, in recent experiments [11] high values of the squeezing parameter have been achieved. We note [cf. Eqs. (9), (10), and (15)] that if the squeezing is not very high then we need to use smaller detection efficiencies. Our proposal contrasts with previous ones [7,12] which used classical Gaussian beams and a birefringent medium.

In Fig. 1, we show a schematic arrangement for realization of the weak values using entangled photons. The entangled photons are generated by an optical parametric amplifier (OPA). In the OPA the pump field interacts nonlinearly in an optical crystal having second-order nonlinearity. As a result of annihilation of one photon of the pump field two entangled photons propagating in two different directions are generated simultaneously. In our scheme, we consider that the signal mode is initially in a coherent state $|\alpha\rangle$ while the idler is initially in vacuum. The photons generated in the signal mode produce excitation [13] in the coherent field $|\alpha\rangle$ present initially. If n photons are generated in the idler mode, the state of the signal mode will be an n-photon-added coherent state. In our scheme, we perform weak detection of the idler photons by using a low-efficiency detector which requires a large number of photons to be produced in the idler mode. Thus we consider an OPA working under high-gain conditions. We note that a similar arrangement with an OPA under low-gain conditions has been used in a recent experiment by Zavatta *et al.* [14], for generating photon-added coherent states [13]. Using the interaction Hamiltonian for the OPA and under the assumption of no pump depletion, the state of the outgoing signal and idler fields can be written as

$$|\psi\rangle = \exp(ra^\dagger b^\dagger - rab)|\alpha,0\rangle, \tag{1}$$

where r is the gain of the amplifier. Using the Baker-Campbell-Hausdorff identity, Eq. (1) simplifies to

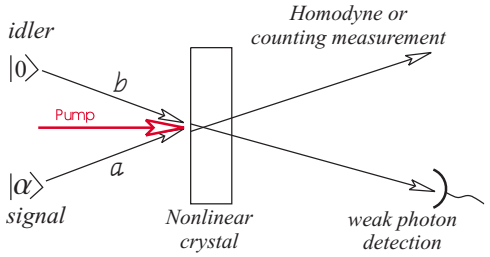

FIG. 1. (Color online) The schematic arrangement for realization of weak values using entangled photons produced in down-conversion. The idler photon is detected with varying efficiency.

$$|\psi\rangle = \exp(\tanh r a^\dagger b^\dagger)\exp[-\ln\cosh r(a^\dagger a + b^\dagger b + 1)] \times \exp(-\tanh r a b)|\alpha,0\rangle = \frac{e^{-|\alpha|^2\tanh^2 r/2}}{\cosh r}\exp(\tanh r a^\dagger b^\dagger)|\alpha',0\rangle, \quad (2)$$

where $\alpha' = \alpha/\cosh r$. Equation (2) shows how the OPA generates a correlated pair of photons, one in the signal mode and one in the idler mode, simultaneously. According to the von Neumann postulate the measurement of the state of the idler mode in the n-photon Fock state $|n\rangle$ would project the state of the signal mode to an n-photon-added coherent state $a^{\dagger n}|\alpha'\rangle$. However, we now follow the idea of Aharonov *et al.* on weak measurements. We measure the idler field weakly, i.e., the measurement does not make the idler field collapse into a single Fock state, with a definite number of photons, but to a probabilistic mixture of various Fock states of different numbers of photons. The weak detection is performed by a low-efficiency detector [15]. Clearly, the weak measurement of the idler field will project the signal field into a superposition of various photon-added coherent states [13]. We now show how the weak detection of idler photons leads to unexpectedly large values of signal field. The density matrix for signal-idler fields is

$$\rho = |\psi\rangle\langle\psi|, \quad (3)$$

where $|\psi\rangle$ is given by Eq. (2). We detect the idler field in the n-photon Fock state $|n\rangle$ by using a detector of quantum efficiency η. The projected state of the signal field is

$$\rho_n^{(s)} = A\sum_{m=n}^{\infty}\binom{m}{n}\eta^n(1-\eta)^{m-n}\langle m|\rho|m\rangle, \quad (4)$$

where A is the normalization constant. Using (2) and (3) and Eq. (4) takes the form

$$\rho_n^{(s)} = N\sum_{m=n}^{\infty}\binom{m}{n}\eta^n(1-\eta)^{m-n}\frac{\tanh^{2m} r}{m!}a^{\dagger m}|\alpha'\rangle\langle\alpha'|a^m, \quad (5)$$

where N is a new normalization constant and the constant term $e^{-|\alpha|^2\tanh^2 r}/\cosh^2 r$ has been absorbed in N. From Eq. (5), it is clear that, because of the nonunity quantum efficiency of the detector, the measurement of the idler field cannot project the signal field onto one of its eigenstates. The projected state of the signal field is a superposition of various eigenstates. Further, for smaller values of η and larger values of the OPA gain parameter r, many eigenstates in the superposition contribute significantly.

It should be noted here that in our scheme we do not perform a measurement on a two-state system as discussed by Aharonov *et al.* [1] in their original proposal. We perform a measurement on an infinite-dimensional system. Here we are particularly interested in the detecting the idler field in the vacuum state. Note that the detection of the idler in the vacuum state for a range of values of the efficiency is enough to reconstruct the full idler field [10]. From Eq. (5), the weak measurement of the idler field in the state $|0\rangle$ projects the signal field onto the state

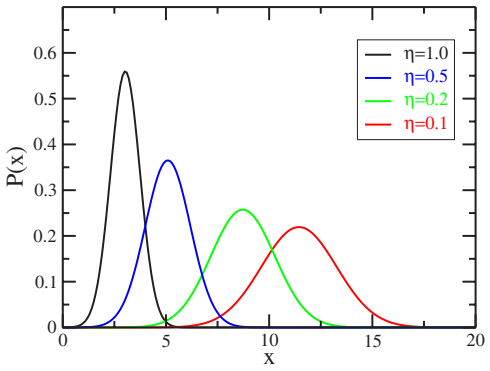

FIG. 2. (Color online) Quadrature distribution of the signal field after measuring the idler photons in the vacuum state by using a detector of efficiency η. Curves from left to right correspond to $\eta = 1.0$, 0.5, 0.2, and 0.1.

$$\rho_0^{(s)} = N\sum_{m=0}^{\infty}(1-\eta)^m\frac{\tanh^{2m} r}{m!}a^{\dagger m}|\alpha'\rangle\langle\alpha'|a^m. \quad (6)$$

The above conditional state of the signal field can be measured either through the photon number distribution or via the quadrature distribution. We next calculate these and show how the weak values get reflected in such distributions.

The quadrature distribution of the projected signal field (6), when the idler field is detected in the vacuum state by using a detector of quantum efficiency η, is given by

$$P_0(x) = N\sum_{m=0}^{\infty}(1-\eta)^m\frac{\tanh^{2m} r}{m!}\langle x|a^{\dagger m}|\alpha'\rangle\langle\alpha'|a^m|x\rangle, \quad (7)$$

where $|x\rangle$ is the eigenstate in the quadrature space. A long calculation leads to the following compact expression for the quadrature distribution of the signal field:

$$P_0(x) = \sqrt{\frac{1-\epsilon}{\pi(1+\epsilon)}}\exp\left[-\frac{1-\epsilon}{1+\epsilon}\left(x - \frac{\sqrt{2}\alpha'}{1-\epsilon}\right)^2\right], \quad (8)$$

where $\epsilon = (1-\eta)\tanh^2 r$. From Eq. (8), it is clear that the projected state of the signal field (6) has Gaussian quadrature distribution. The peak of the distribution appears at

$$x = \sqrt{2}\alpha'/(1-\epsilon), \quad (9)$$

and the width of the distribution δx is given by

$$2(\delta x)^2 = \frac{1+\epsilon}{1-\epsilon}. \quad (10)$$

It is clear from Eqs. (9) and (10) and that for a low-efficiency detector ($\eta \ll 1$) and high-gain OPA ($r > 1$), as the value of ϵ tends toward 1, a peak in the quadrature distribution occurs for exceptionally large values of x. Further, the width of the distribution also becomes very large for these values of the parameters. Interestingly enough, in our model the width of the distribution also depends on the weakness of the measurement.

In Fig. 2, we show the quadrature distributions of the projected states of the signal field after detecting the idler field in the vacuum state. For 100% detection efficiency the

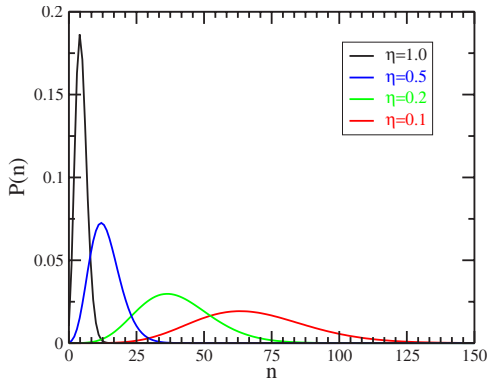

FIG. 3. (Color online) Photon distribution of the signal field after measuring the idler photons by using a detector of efficiency η. The idler field is detected in the vacuum state $|0\rangle$. Curves from left to right correspond to $\eta=1.0$, 0.5, 0.2, and 0.1.

maximum in the quadrature distributions occurs at $x\approx 3$, corresponding to the value $x=\sqrt{2}\alpha'$, where $\alpha'=\alpha/\cosh r$, $\alpha=5$, and $r=1.5$. We find that, for lower detection efficiency, the maximum in the quadrature distribution shifts to exceptionally larger values of x. For $\eta=0.1$ the maximum in the x quadrature appears around $x\approx 12$. Further, the spread in the distribution becomes very large for such smaller values of η. This is a remarkable realization of the idea of Aharonov *et al.* using entangled photons.

In order to understand the exact nature of the weak values we look at Eq. (6) for the projected state of the signal field. Clearly, the projected state of the signal field is a superposition of photon-added coherent states $a^{\dagger m}|\alpha'\rangle$ generated by successive addition of the photons in the signal mode. The amplitude of the mth term in Eq. (6) is proportional to $\epsilon^m/m!$, where $\epsilon=(1-\eta)\tanh^2 r$. For $\eta=0.1$ and $r=1.5$, as the value of ϵ is 0.74, the amplitude of the fifth term is of the order of 10^{-3}. Further, the higher-order terms will have much smaller amplitude and can be neglected. The quadrature distribution of the five-photon-added coherent state $a^{\dagger 5}|\alpha'\rangle$ will have a maximum at $x\approx\sqrt{2}\sqrt{|\alpha'|^2+5}$. Thus the highest-order contributing eigenstate of the signal field has a maximum at $x\approx 4.5$. In Fig. 3 the maximum in the quadrature distribution corresponding to these parameters occurs at $x\approx 12$, which is exceptionally large, and there is no doubt that the projected values of the signal field in our scheme are weak values. The exceptional displacement in the maximum of the quadrature distribution occurs as a result of interferences between various states contributing to the projected state of the signal field. Further, it should also be noted that the photon-added coherent states $a^{\dagger m}|\alpha'\rangle$ show more and more squeezing in their quadrature on increasing m [13], while the projected state of the signal field exhibits broadening in the quadrature distribution. Clearly, choosing smaller detection efficiencies (a few percent), which are definitely feasible [10], would lead to larger displacement and larger fluctuations.

Next we show how the weak measurements get reflected in the photon number distribution of the signal field. The photon distribution of the projected state of the signal field (6) is calculated as follows:

$$P_0(n)=N\sum_{m=0}^{\infty}(1-\eta)^m\frac{\tanh^{2m}r}{m!}\langle n|a^{\dagger m}|\alpha'\rangle\langle\alpha'|a^m|n\rangle, \tag{11}$$

$$P_0(n)=N(1-\eta)^n\tanh^{2n}r \times\sum_{m=0}^{n}\frac{n!}{m!(n-m)!^2}\left(\frac{\alpha'^2}{(1-\eta)\tanh^2 r}\right)^{n-m}. \tag{12}$$

Using the definition of Laguerre polynomials and evaluating the normalization constant, Eq. (12) takes the form

$$P_0(n)=(1-\epsilon)e^{-\alpha'^2/(1-\epsilon)}\epsilon^n L_n\left(-\frac{\alpha'^2}{\epsilon}\right), \tag{13}$$

where $L_n(q)$ is the Laguerre polynomial of order n. The photon distributions of the projected signal state (6) are shown in Fig. 3. For unity detection efficiency the field has a maximum at $n\approx 5$ corresponding to the coherent state $|\alpha'\rangle$. As the detection efficiency η decreases the peak in the distribution moves very fast toward higher values of n and the width of the distribution also increases. As we have discussed earlier, for $\eta=0.1$, only terms up to $m=5$ can contribute significantly in the projected signal state (6). Thus the signal field contains its highest-order eigenstate having a maximum in the photon distribution at $|\alpha'|^2+5\approx 10$. But the actual weak value of the maximum photon numbers in the distribution occurs at $n\approx 75$.

To further probe the field statistics of the projected signal states in weak measurement, we calculate the Mandel Q parameter defined by

$$Q=\frac{\langle n^2\rangle-\langle n\rangle^2}{\langle n\rangle}-1, \tag{14}$$

where $\langle n\rangle$ is the average number of photons in the projected state of the signal field. The average number of photons for state (6) is

$$\langle n\rangle=\frac{\epsilon-\epsilon^2+\alpha'^2}{(1-\epsilon)^2}. \tag{15}$$

It is clear from Eq. (15) that the average number of photons becomes very large for $\epsilon\to 1$ for smaller values of η. The calculated value of the Mandel Q parameter for the state (6) is

$$Q=\frac{(\epsilon-\epsilon^2+\alpha'^2)(1-\epsilon+\alpha'^2)-\alpha'^4}{(1-\epsilon)^2(\epsilon-\epsilon^2+\alpha'^2)}-1. \tag{16}$$

In Fig. 4, we plot the Mandel Q parameter for the signal state (6) with respect to the efficiency of the detector used to measure the idler field. For smaller values of detection efficiency the Q parameter has large positive values and the states of the signal field follow super-Poissonian statistics. As the detector efficiency increases the value of the Q parameter decreases. For the detector efficiency more than 0.9 the Q parameter for the state (6) is zero, which reflects that the projected state of the signal field is the coherent state $|\alpha'\rangle$.

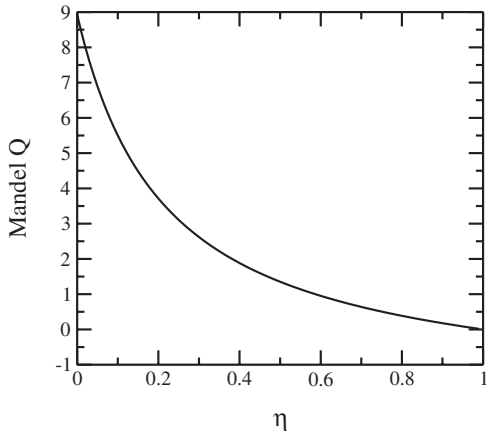

FIG. 4. Value of Mandel's Q parameter for the signal field after detecting the idler field in the vacuum state.

Next we calculate the Wigner distribution of the projected state of the signal field. The Wigner distribution for the state having density matrix ρ can be obtained using coherent states from the formula

$$W(\gamma) = \frac{2}{\pi^2} e^{2|\gamma|^2} \int \langle -\beta|\rho|\beta\rangle e^{-2(\beta\gamma^* - \beta^*\gamma)} d^2\beta. \quad (17)$$

For state (6) the Wigner function is found to be

$$W_0(\gamma) = \frac{2(1-\epsilon)}{\pi(1+\epsilon)} \exp\left[-\frac{2(1-\epsilon)}{1+\epsilon} \left| \gamma - \frac{\alpha'}{1-\epsilon} \right|^2 \right]. \quad (18)$$

The Wigner distribution of the state (6) is a Gaussian whose width is greater than the width of the distribution associated with a coherent state. Hence the Glauber-Sudarshan distribution is also a well-defined Gaussian with a width $\epsilon/(1-\epsilon)$ and centered at $\alpha'/(1-\epsilon)$. The Wigner function shifts to larger values and broadens as the detection efficiency goes down.

In conclusion, we have shown how one can use entangled photon pairs produced in a high-gain parametric amplifier and imperfect measurements on the idler field to realize the idea of weak values of the observables at the level of quantized fields. We show how the weak measurements of the idler field produce exceptionally large changes in the quantum state of the signal field. We show large changes in both the mean values of the observables as well as in the fluctuations. For illustration purposes we have chosen to detect the idler field in the vacuum state. We could choose to measure the idler in some other state. This would lead to similar results. We add that detection of the idler field in a single-photon state produces a nonclassical character of the signal field.

The authors thank NSF (Grant No. CCF 0524673) for supporting this work. G.S.A. also thanks Marco Bellini for interesting correspondence.

[1] Y. Aharonov, D. Z. Albert, and L. Vaidman, Phys. Rev. Lett. **60**, 1351 (1988).
[2] J. Von Neumann, *Mathematical Foundations of Quantum Mechanics* (Princeton University Press, Princeton, NJ, 1996).
[3] I. M. Duck, P. M. Stevenson, and E. C. G. Sudarshan, Phys. Rev. D **40**, 2112 (1989).
[4] L. M. Johansen, Phys. Rev. Lett. **93**, 120402 (2004).
[5] J. M. Knight and L. Vaidman, Phys. Lett. A **143**, 357 (1990); Y. Aharonov and L. Vaidman, Phys. Rev. A **41**, 11 (1990); Y. Aharonov, S. Popescu, D. Rohrlich, and L. Vaidman, *ibid.* **48**, 4084 (1993).
[6] J. Ruseckas and B. Kaulakys, Phys. Rev. A **66**, 052106 (2002); H. M. Wiseman, *ibid.* **65**, 032111 (2002).
[7] N. W. M. Ritchie, J. G. Story, and R. G. Hulet, Phys. Rev. Lett. **66**, 1107 (1991).
[8] Q. Wang, F. W. Sun, Y. S. Zhang, Jian-Li, Y. F. Huang, and G. C. Guo, Phys. Rev. A **73**, 023814 (2006); S. E. Ahnert and M. C. Payne, *ibid.* **69**, 042103 (2004).
[9] A. Parks, D. Cullin, and D. Stoudt, Proc. R. Soc. London, Ser. A **454**, 2997 (1998); G. J. Pryde, J. L. O'Brien, A. G. White, T. C. Ralph, and H. M. Wiseman, Phys. Rev. Lett. **94**, 220405 (2005).
[10] G. Zambra, A. Andreoni, M. Bondani, M. Gramegna, M. Genovese, G. Brida, A. Rossi, and M. G. A. Paris, Phys. Rev. Lett. **95**, 063602 (2005).
[11] M. Caminati, F. De Martini, R. Perris, F. Sciarrino, and V. Secondi, Phys. Rev. A **73**, 032312 (2006).
[12] N. Brunner, V. Scarani, M. Wegmuller, M. Legre, and N. Gisin, Phys. Rev. Lett. **93**, 203902 (2004); D. R. Solli, C. F. McCormick, R. Y. Chiao, S. Popescu, and J. M. Hickmann, *ibid.* **92**, 043601 (2004).
[13] G. S. Agarwal and K. Tara, Phys. Rev. A **43**, 492 (1991).
[14] A. Zavatta, S. Viciani, and M. Bellini, Science **306**, 660 (2004).
[15] There are methods (Ref. [10]) to simulate low efficiencies even when actually using high-efficiency detectors. In fact, in the experiments of Zambra *et al.* efficiencies starting from nearly zero to 66% were used.